

Monolithic Colliding-Pulse Mode-Locked Quantum-Well Lasers

Young-Kai Chen, *Member, IEEE*, and Ming C. Wu, *Member, IEEE*

Invited Paper

Abstract—Integration of the whole mode-locked laser onto a single piece of semiconductor offers a great deal of advantages, including total elimination of optical alignment processes, improved mechanical stability, and the generation of short optical pulses at much higher repetition frequencies. We utilize the semiconductor laser processing technologies to implement the colliding-pulse mode-locking (CPM) scheme, which is known to effectively shorten the pulses and increase stability, on a miniature monolithic semiconductor cavity. In this paper, we review the principles and recent progress of monolithic colliding-pulse mode-locked quantum-well lasers.

I. BACKGROUND

RECENT advances in the areas of high bit rate time-division multiplexed communication systems with external modulation, ultralong distance soliton fiber transmission experiments [1, 2], picosecond optical logic gates [3]–[5], optoelectronic sampling systems [6], and broad-band submillimeter-wave generation [7] require very short optical pulses with pure spectral properties. In order to realize these systems, a compact, stable, and reliable optical source is highly desirable. Theoretically, it is possible to generate very short optical pulses (~ 50 fs) in semiconductor gain medium because of its broad gain spectrum (~ 1000 Å). Over the past decades, the reliability and compactness of semiconductor diode lasers have been well proven and implemented in today's communication systems. In this paper, we utilize the semiconductor quantum-well diode laser technologies to generate short optical pulses with excellent spectral purity and tuning capability on their lasing characteristics.

Gain switching and mode locking are two commonly used methods to generate short optical pulses from semiconductor lasers. Gain switching of a laser diode is easily achieved by capitalizing the first period of the relaxation oscillation which is generated by switching on a diode laser biased just below threshold [8]–[10]. The advantage of using the gain-switched pulses is the flexibility to change the repetition rate without modifying the cavity length. However, when the laser is suddenly switched from below to above threshold, significant fluctuations in both the carrier density and the time delay between the

excitation and optical output are produced. These produce significant frequency chirp [11] and timing jitter [12] associated with the gain-switched optical pulses.

Short optical pulses with very pure spectral properties and low timing jitter can be obtained by mode-locked semiconductor lasers. Earlier works have successfully replaced the gain and absorption media such as dyes with compact semiconductors in implementing active (forced) mode-locked, passive mode-locked, and hybrid mode-locked lasers using external resonant cavities and bulk optical elements [13]. Active mode locking generates accurately timed pulses and provides synchronization between electrical clocks and optical pulses. By using a stable microwave oscillator to modulate an intracavity gain, loss, or phase element at the intercavity mode spacing frequency, the longitudinal modes of the laser are phase-locked together to produce short optical pulses. Ho *et al.* reported the first mode-locked semiconductor laser with a pulsewidth of 23 ps [14]. A shorter pulsewidth of 0.58 ps was obtained by modulating the laser at higher harmonics of the fundamental cavity frequency [15]. Lau indicated that narrow-band modulation of semiconductor lasers is possible above 100 GHz at the intercavity mode frequency [16]. Optical pulses with a repetition rate up to 100 GHz have been generated with passive mode-locked tandem-contact semiconductor lasers [17], [18]. Practically, it is difficult to couple the modulation signal to the device at high frequency because of parasitics. In order to synchronize the pulses at a high repetition rate, the hybrid mode-locking technique is very useful [19]. In hybrid mode locking, an intracavity saturable absorber shortens the pulses and brings the laser close to the passive mode-locking condition. Shorter pulses and less RF driving power can be obtained. A pulsewidth of 1.4 ps was reported from a monolithic hybrid mode-locked semiconductor laser at 15 GHz [20].

An intracavity saturable absorber sharpens the leading edge of the recirculating pulses by preferentially passing the high energy peak of the pulses with minimum loss. In order to obtain a net reduction of pulsewidth over a round-trip through the gain and absorber elements, the recovery of the absorber saturation must occur faster than that of the gain. The peak portion of the pulse sees a net gain because of the smaller gain cross section, while the trailing edge of the pulse is sharpened by the fast recovery

Manuscript received March 11, 1992.

The authors are with AT&T Bell Laboratories, Murray Hill, NJ 07974.
IEEE Log Number 9202060.

0018-9197/92\$03.00 © 1992 IEEE

time of the absorber [21]. The pulse shaping process continues until it is limited by the pulse-broadening (dispersive) mechanisms inside the cavity. Because the pulse-shaping mechanisms are determined by the difference in transient saturation and recovery time constants between the gain and absorber, it is possible to generate short optical pulses with a repetition rate beyond the relaxation oscillation frequency of the semiconductor laser.

The colliding-pulse mode-locking (CPM) scheme has been widely used to generate ultrashort transform-limited pulses in dye lasers [22], [23]. Instead of having a single pulse passing through the saturable absorber at one time, CPM lasers utilize the coherent interaction of two counter-propagating pulses colliding at the saturable absorber to produce shorter pulses [24], [25]. The two counter-propagating pulses time themselves to collide in the saturable absorber because less energy is lost. Compared to a single pulse traveling in the cavity, the pulse shaping is more effective with the CPM configuration because there are two pulses added coherently to saturate the absorber while there is only one pulse to saturate the gain section. This enhanced effective saturation cross section of the absorber helps to stabilize and shorten the pulses. In this paper, we exploit the multiple quantum-well (MQW) semiconductor laser technology to implement the CPM configuration on a single chip.

II. DEVICE STRUCTURE

Previously, colliding-pulse mode-locked semiconductor lasers were implemented using degraded semiconductor in external ring or linear cavities [26], [27]. One major problem associated with the external cavity configuration is the intracavity reflection from nonideal antireflection-coated facet interfaces. Instead of a single pulse repeating at the round-trip time of the external cavity, bursts of pulses are generated from this interface [15], [26]. The mechanical alignment and thermal stability of each optical element also make the whole system very difficult to use. The use of an integrated waveguide cavity in a semiconductor laser removes the uncontrollable multiple-pulse bursts in mode-locked lasers with external cavities [28].

Degraded semiconductors were utilized to shorten the lifetime of saturable absorbers [26], [29]. Saturable absorbers obtained through this process were unstable and not reliable for practical system applications. Over the past decade, the optical properties of semiconductor quantum wells have been studied extensively [30]–[32]. Their unique properties such as high differential gain, low dispersion, broad-gain spectrum, nonlinear gain-saturation characteristics, and the fast recovery time enable them to be used as the gain and absorber media to generate short mode-locked pulses. Recently, very short and high power optical pulses have been generated in mode-locked lasers using semiconductor MQW epilayers as saturable absorber inside an external cavity. However, the output pulses from the cavity were strongly chirped, and extensive chirp compensation and pulse compression tech-

niques were needed to shorten the pulses outside the laser cavity. For example, Delfyett *et al.* reported 0.46 ps pulses with a peak power of 70 W at 828 nm, which was amplified and compressed from the 5 ps pulses emitting from the cavity with 800 μ W averaged power [33]. Xiang *et al.* demonstrated 0.153 ps pulses with peak power exceeding 1 kW by chirp compensating the 21 ps output pulses with a pair of diffraction gratings [34].

The inhomogeneously pumped semiconductor laser with tandem contacts utilizes the same medium under different bias conditions to provide both saturable absorption and gain functions [16]. As shown in Fig. 1, if the absorber is biased at a lower pumping level than the gain section, the saturation cross section of the absorber element is larger than that of the gain element. This constitutes a necessary condition for the generation of stable passive mode-locked pulses. Recently, the gain recovery dynamics in semiconductor laser amplifiers has been studied with ultrafast pump-probe techniques using femtosecond optical pulses [35]–[38]. After a short optical pulse traversing the active semiconductor medium, the gain is depleted by the stimulated emission and the redistribution of free carriers. The recovery of the gain depends on the carrier cooling processes, initial carrier concentration (i.e., the bias condition of the medium), and carrier-storage reservoir of the waveguide structure. The observed recovery process usually consists of a very fast subpicosecond time constant associated with the carrier cooling process and a 1.7–7 ps time constant from the carrier diffusion. The fast relaxation dynamics of the semiconductor multiple quantum wells allows the generation of short pulses at very high repetition frequency. Together with the low loss and low frequency chirp properties of the waveguide, the MQW semiconductor laser structure meets the necessary criteria to implement monolithic mode-locked lasers.

Fig. 2 shows the epitaxial layer structure of the monolithic CPM lasers. The lasers are fabricated with an InGaAsP buried heterostructure (BH) graded index separate confinement heterostructure (GRIN-SCH) lattice-strained MQW structure prepared by a two-step organometallic vapor phase epitaxy (OMVPE) growth technique. In the first growth, the lower part of InGaAsP graded index confining layers are deposited on top of a 2 μ m thick n-InP cladding layer with step-wise decreasing band-gap layers with band-gap wavelengths of 1.08 μ m (25 nm thick), 1.16 μ m (25 nm thick), and 1.25 μ m (25 nm thick), and followed by five InGaAs strained quantum wells (5 nm thick) and InGaAsP quaternary barriers with a band-gap wavelength of 1.25 μ m (22.5 nm thick). The lasing wavelength is 1.55 μ m. The upper InGaAsP graded index confining layers, similar to the lower part, are then grown with increasing bandgaps, and followed by a 2 μ m thick p-InP cladding layer and a 120 nm thick p⁺-InGaAsP contact layer (Zn doped to 5×10^{18} cm⁻³). After 1 μ m wide continuous waveguide strips are formed by etching down to the lower n-cladding layer with SiO₂ mask, the iron-doped semi-insulating InP layer is selec-

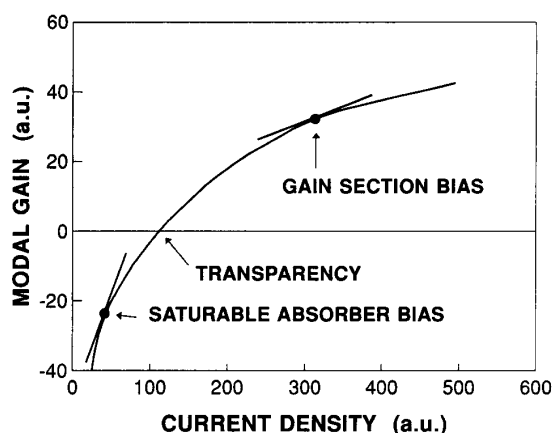


Fig. 1. The saturation characteristics of semiconductor quantum wells. The cross section of the absorber is larger than that of the gain bias condition, which constitutes the necessary condition for passive mode locking.

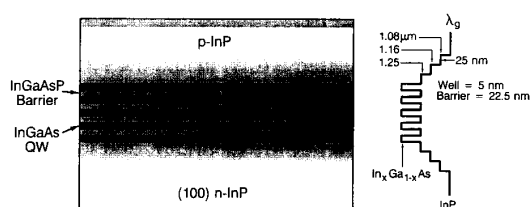


Fig. 2. The epitaxial layer structure used to fabricate monolithic colliding-pulse mode-locked quantum-well lasers.

tively grown around the waveguide strips to provide electrical isolation and optical confinement. Detailed growth conditions and device performance of the MQW lasers were reported in [39]. Standard lithography and wet chemical etching are used to construct the final structure.

III. MONOLITHIC PASSIVE CPM LASERS

The schematic diagram of the monolithic passive CPM laser is depicted in Fig. 3 [40]. The continuous GRIN-SCH quantum-well region extends through the entire cavity to remove undesired waveguide mismatches. The saturable absorber is located at the symmetry center of the cavity in order to maximize the coherent coupling between the two colliding pulses [25]. The remaining two sections are electrically connected together and forward biased to provide gain. The electrical isolation between contact metals is achieved by removing the heavily doped top p-type contact epitaxial layer with wet chemical etching. The length of the saturable absorber is 15 μm for lasers with 0.25 mm cavity length, and is 50 μm for other cavity lengths. Typical resistance between the 10 μm gap is 1 K Ω . Because there are two counter-propagating pulses traveling simultaneously in the cavity, the fundamental repetition rate in the CPM configuration is twice of the round-trip frequency of the whole cavity. Devices of cavity length of 2.1, 1.0, 0.534, and 0.25 mm are fabricated to generate optical pulses with repetition rates of 40, 80,

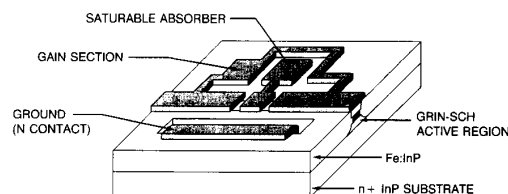


Fig. 3. The schematic diagram of the passive monolithic colliding-pulse mode-locked quantum-well laser. The saturable absorber is located at the center of the linear cavity with the remaining cavity as the gain sections. Only two dc power supplies are needed to generate passive mode-locked pulses.

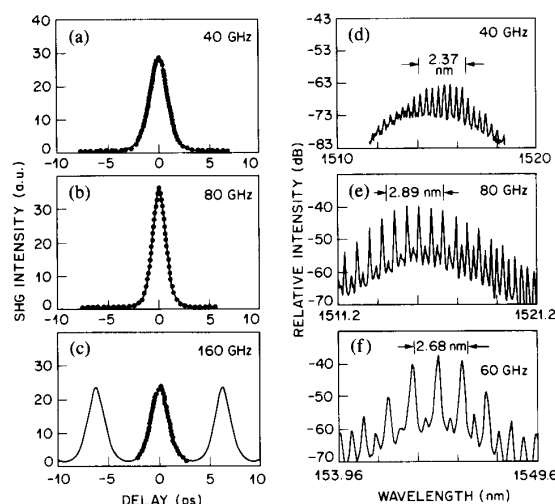


Fig. 4. The SHG autocorrelation traces of the pulses from passive monolithic CPM lasers of various cavity lengths (a) 2.1 mm, (b) 1.0 mm, and (c) 534 μm . The simulated SHG autocorrelation traces (solid curves) agree well with the measured traces (dots) using a hyperbolic-secant pulse shape with transform-limited pulsewidths of 1.1, 0.83, and 1.0 ps, respectively. The mode-locked optical spectra are simultaneously recorded in (d), (e), and (f), respectively. Because of the CPM configuration, the corresponding optical pulse repetition rates are 40, 80, and 156 GHz, respectively. The optical modulation depth is nearly 100%.

156, and 350 GHz, respectively. Typical continuous-wave (CW) threshold current is 50 mA for a 2.1 mm long laser at room temperature.

Fig. 4 (a)–(c) shows the noncollinear second harmonic generation (SHG) autocorrelation traces (dots) from the monolithic passive CPM lasers with cavity lengths of 2.1 mm, 1.0 mm, and 534 μm , respectively. Their optical spectra are recorded in Fig. 4 (d)–(f). Using a hyperbolic-secant pulse waveform, the simulated SHG autocorrelation traces [solid curves in Fig. 4 (a)–(c)] fit very well with the measured data. The extinction ratios are better than 95%, and only a single pulse is observed for each cycle. The full width at half maximum (FWHM) pulsewidths of 1.1, 0.83, and 1.0 ps are obtained for CPM lasers with cavity length of 2.1 mm, 1.0 mm, and 534 μm , respectively. From the measured FWHM spectral widths in Fig. 4 (d)–(f), time-bandwidth products ($\Delta\tau \times \Delta\nu$) are 0.34, 0.31, and 0.34, respectively, which are very close to the transform-limited value of 0.31 for hyperbolic-secant pulses.

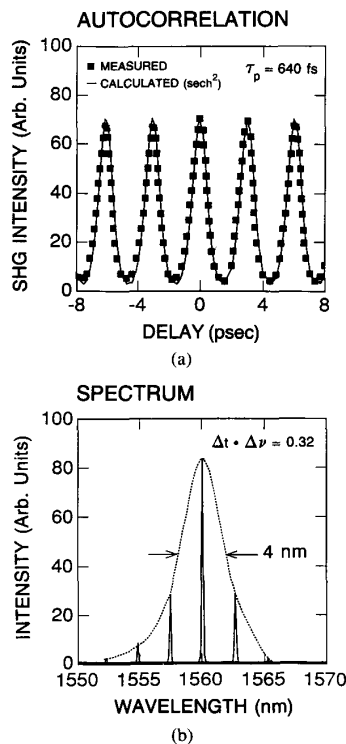


Fig. 5. (a) Measured (dots) and simulated (solid curves) SHG autocorrelation traces of the passive CPM laser with a cavity length of $250 \mu\text{m}$ show optical pulses with FWHM pulsewidth of 640 fs at 350 GHz. A hyperbolic secant pulse shape is used in the simulation. (b) The time-averaged optical spectrum shows a FWHM bandwidth of 4 nm which corresponds to a nearly transform-limited time-bandwidth product of 0.32.

By shortening the cavity length to $250 \mu\text{m}$, we are able to obtain subpicosecond pulses at 350 GHz. Because of the large mirror loss in a short cavity laser, the length of the saturable absorber is reduced. Fig. 5(a) shows the measured (dots) and calculated (curve) SHG autocorrelation trace of this short cavity CPM laser. It shows a very good fit with a hyperbolic secant pulse shape, and the pulse width is 640 fs. The measured FWHM spectral width is 4 nm [Fig. 5(b)], which indicates these optical pulses are transform limited with a time-bandwidth product of 0.32. To effectively sharpen the optical pulses, the physical length of the saturable absorber should be shorter than the optical pulses. It takes almost 1 ps to traverse a $50 \mu\text{m}$ saturable absorber and two $10 \mu\text{m}$ long gaps, or 0.5 ps for the $15 \mu\text{m}$ long saturable absorber and gaps. The effect of the length of the saturable absorber on the pulse width of the 0.25 mm long CPM laser is shown in Fig. 6. A minimum pulsewidth of 610 fs is obtained in this experiment.

IV. MONOLITHIC HYBRID CPM LASERS

In many applications, it is necessary to synchronize optical pulses to electrical clocks. This can be achieved by hybrid mode locking. The schematic diagram of the monolithic hybrid CPM laser is depicted in Fig. 7 [41].

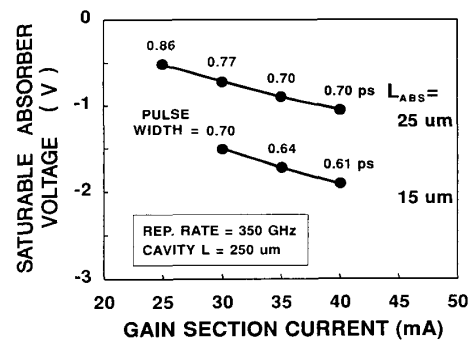


Fig. 6. The optimal bias conditions for short pulse generation from $250 \mu\text{m}$ long CPM lasers with 10 and $15 \mu\text{m}$ long saturable absorbers.

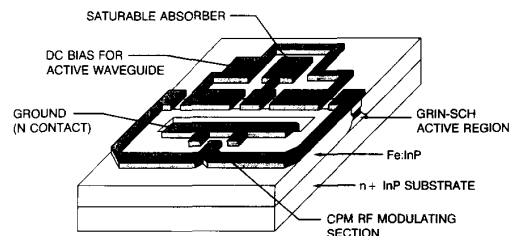


Fig. 7. The schematic diagram of the hybrid monolithic colliding-pulse mode-locked quantum-well laser. A pair of $70 \mu\text{m}$ long modulator sections are separated from the gain section in order to synchronize optical pulses with the external microwave sources.

The cavity is divided into five sections with two extra sections added near the facets as modulators. The lengths of the modulator sections and the saturable absorber are $70 \mu\text{m}$. In this monolithic hybrid CPM laser, an external RF source is used to actively mode lock two counter-propagating pulses in the linear cavity. The timing accuracy between the two modulators is maintained by the equal path length of the integrated transmission line, which is defined by accurate photolithographic process.

Fig. 8 shows the measurement arrangements to characterize the monolithic CPM laser. The laser is driven by the amplified signal from a RF network analyzer which sweeps from dc to 20 GHz to locate the cavity resonant frequency. The emitted light is distributed to an autocorrelator, an optical spectrum analyzer, and a high-speed PIN detector connected to the receiver port of the network analyzer. By injecting small-signal RF current into the modulators, the frequency response of a 2.1 mm long laser is shown in Fig. 9. As shown in Fig. 9(a), a Fabry-Perot cavity resonant peak can be clearly seen at 19.2 GHz when the whole cavity is uniformly biased. However, when a negative bias of -0.4 V is applied to the saturable absorber, the laser operates close to passive CPM regime and the resonant peak is suppressed by 20 dB [Fig. 9(b)]. Once the cavity resonant frequency is located, the RF analyzer is then switched to the CW mode with its frequency set to twice the cavity resonant frequency. The influence of the RF power on the time-average optical spectrum of a 2.54 mm long CPM laser is illustrated in

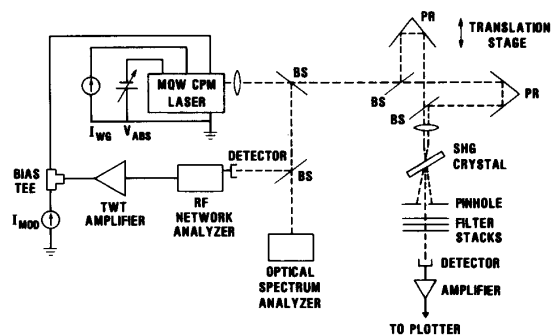


Fig. 8. The experimental arrangement to characterize the monolithic hybrid mode-locked CPM laser.

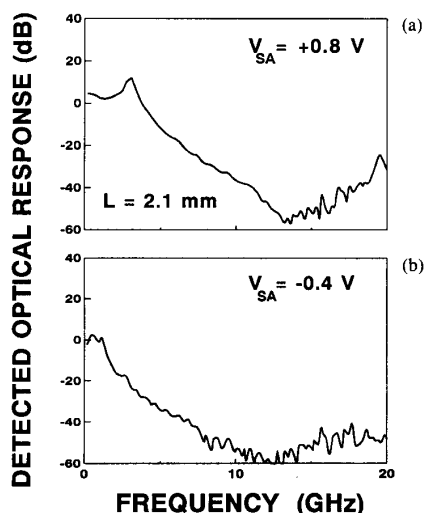


Fig. 9. The small-signal frequency response of the 2.1 mm long monolithic hybrid CPM laser (a) under uniform injection and (b) close to passive mode locking. The fundamental Fabry-Perot cavity resonant peak is suppressed by more than 20 dB when the laser is operated near passive mode locking.

Fig. 10. At -25 dBm of RF power, there is a dominant single longitudinal mode. The peak height of the dominant mode is suppressed, as the RF power increases. At $+10$ dBm (trace 07), a series of longitudinal modes with heights reduced by more than 10 dB is observed. The spectral width broadens to a few nm and the peak wavelength is shifted to the longer wavelength.

Fig. 11 shows the temporal response of the 2.1 mm long CPM laser recorded by a synchron-scan streak camera. Driven at 38.5 GHz, it shows a FWHM pulsewidth of 5.96 ps with nearly 100% modulation depth. This pulsewidth is limited by the resolution of the streak tube and timing jitters from the synchronizing electronics. Using a noncollinear second harmonic generation autocorrelator with 5 mm thick LiNbO_3 crystal, more accurate temporal pulse shape measurements are performed. The influence of saturable absorber bias on the pulse shape is illustrated in Fig. 12. The power from the RF amplifier is fixed at 25 dBm. As the negative bias on the absorber

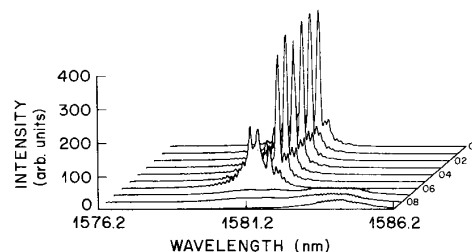


Fig. 10. The influence of the RF driving power on the optical spectrum of a 2.54 mm long monolithic hybrid CPM laser. The RF power starts at -25 dBm (Trace 00) and increases by steps of 5 dBm. The mode-locked spectrum starts to appear for power beyond 10 dBm.

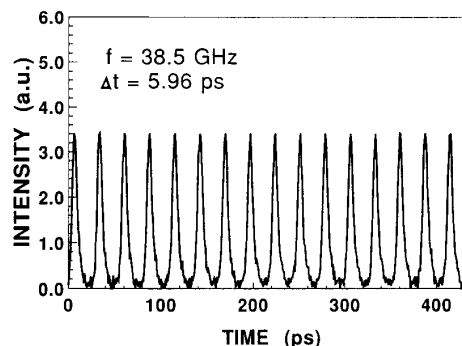


Fig. 11. The temporal response of a 2.1 mm long monolithic hybrid CPM laser with a repetition rate of 38.5 GHz recorded by a synchron-scan streak camera.

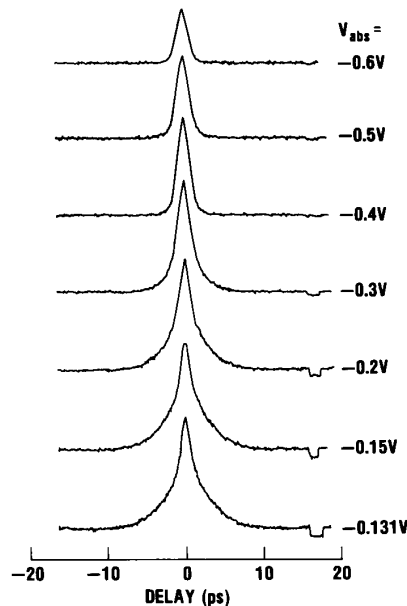


Fig. 12. The influence of the saturable absorber bias on the SHG autocorrelation traces. The 2.1 mm long laser is driven under a fixed RF power of 25 dBm at 38.5 GHz.

increases, the dc component decreases and the pedestal of the pulse envelope narrows down. When the absorber is biased below -0.4 V, near transform-limited pulses are

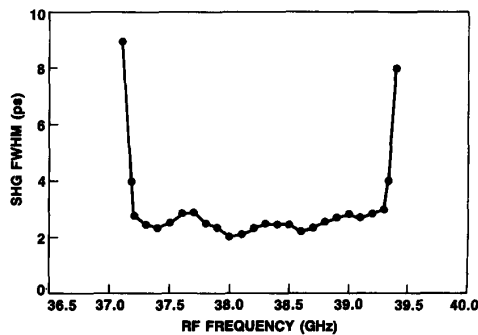


Fig. 13. The SHG autocorrelation pulse width of a 2.1 mm long laser under various microwave driving frequency. A 5% tuning range is obtained.

obtained with very little dc components. The mode-locked SHG autocorrelation trace fits very well to the calculated curve using a hyperbolic secant pulse shape with 0.95 ps pulsewidth. From the 2.6 nm spectral width, the time-bandwidth product ($\Delta t \times \Delta \nu$) is 0.32 which is very close to the transform-limited value of 0.314. Because the waveguide consists of active media, the effective index of the waveguide can be modified by the injected carrier concentration. This provides a small tuning range of the cavity resonant frequency. A 5% tuning range is obtained for this 2.1 mm long CPM laser as shown in Fig. 13.

V. OPERATION RANGES AND STABILITY

A necessary condition for passive mode locking is that the saturable absorber cross section is larger than the gain cross section [21]. However, the same condition is also a necessary condition for self-pulsation. It was concluded that it was very difficult to generate very short pulses without the simultaneous self-pulsating envelope with single pulse tandem-contact mode-locked semiconductor laser [42]. High reflection facet coatings were needed to separate the mode-locking regime from the self-pulsation regime [43]. Because of the enhanced cross section of the saturable absorber in the CPM configuration, we observe a clean mode-locked regime without any self-pulsation.

Depending on the bias conditions of the gain and absorber, the semiconductor CPM laser can operate in several modes: mode-locking, self-pulsating, and CW lasing. Fig. 14 shows the three regimes of operation for different absorber bias voltage (V_{SAT}) and gain section current (I_G) for a passive CPM MQW laser with 1 mm long cavity length. In contrast to the tandem-contact lasers, a clean mode-locked region is observed between the CW and self-pulsation regions. Furthermore, the mode-locked pulses are completely free from self-pulsation, as observed in Fig. 15. Fig. 15 shows the optical output of a 1 mm long passive CPM laser in various bias regions. The optical output is analyzed by a SHG autocorrelator, a high-speed 20 GHz sampling scope, a RF spectrum analyzer, and an optical spectrum analyzer. Under the uniform injection condition, the laser lases in CW mode, and no features are observed by the autocorrelator or sampling

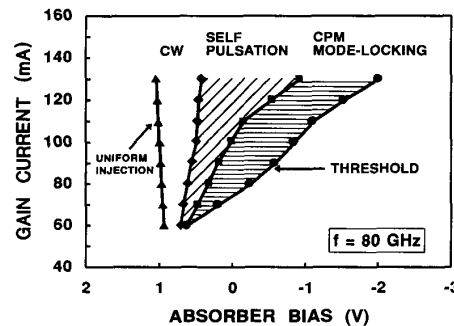


Fig. 14. The experimental bias ranges for a 1 mm long monolithic passive CPM laser to operate in (a) CW lasing, (b) self-pulsating, and (c) mode-locking regimes, respectively. V_{SAT} is the bias voltage on the absorber and I_G is the gain section current.

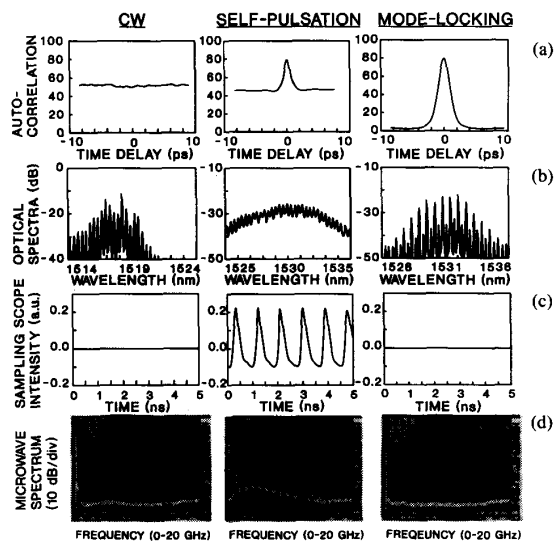


Fig. 15. Simultaneous measurements of the 1 mm long CPM laser with (a) autocorrelator, (b) optical spectrum analyzer, (c) sampling scope, and (d) microwave spectrum analyzer and high speed PIN detector in three operation regions.

scope. The mode spacing of the optical spectrum corresponds to the round-trip time through the whole cavity. When the laser is partially mode locked with a self-pulsating envelope, a coherent spike is observed in the SHG autocorrelation trace with a large dc background, and the time-averaged spectral linewidth is broadened in the optical spectrum. The strong pulsation are visible on the sampling scope as well as the RF spectrum with a repetition rate of 1 GHz. When the laser operates in the mode-locked regime, the autocorrelation trace shows a clean pulse with very low dc background. The pulsewidth is 1.3 ps after the SHG autocorrelation trace is deconvoluted with a hyperbolic secant pulse shape. The spacing between adjacent modes is twice that of a CW laser, which indicates the double-pulse operation in colliding-pulse mode locking. Because the repetition rate is 80 GHz, no structures are observed on either the sampling scope or

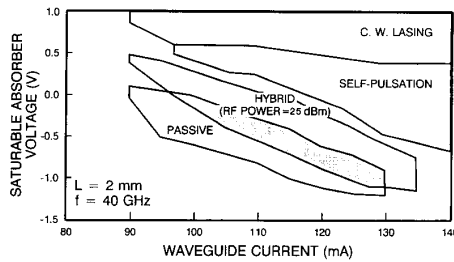


Fig. 16. The experimental bias ranges of 2.1 mm long monolithic CPM laser to operate in CW lasing, self-pulsating, hybrid mode-locking, and passive mode-locking regimes, respectively.

the microwave spectrum analyzer with bandwidths of 20 GHz.

The mode-locking range occurs at lower pump level (less gain current or more negative biased absorber voltage) than that of self-pulsation. This improved mode-locking stability in the CPM configuration is the result of the enhanced saturation cross section from the coherent interference between two colliding pulses in the saturable absorber, as was analyzed theoretically in [25]. The two-pulse CPM configuration is very effective in generating short mode-locked pulses and preventing the occurrence of self-pulsation envelope. The influence of the external microwave modulation on the mode-locking operations is shown in Fig. 16 for a 2.1 mm long CPM laser. In the mode-locked regions, stable optical pulses with less than 1.4 ps pulsewidth and greater than 90% modulation depth are obtained. By adding the active driving source, mode-locked pulses are generated with less reverse bias on the saturable absorber.

VI. TUNING WITH EXTERNAL ELEMENTS

For many applications such as optical solitons and non-linear optical logic devices, optical pulses with high peak power, prescribed wavelength, and pulsewidth are needed. Tuning of the wavelength and pulsewidth allows more flexibility in the design of optical systems. For lasers operating at 1.55 μm , the erbium-doped fiber amplifiers (EDFA) [44] are ideal for amplifying ultrashort optical pulses without distortion because the relaxation time of the EDFA's (~ 1 ms) are much longer than both the pulse duration and the period. In the following, we demonstrate the amplification with EDFA, wavelength tuning, and spectral windowing of the CPM pulses.

A schematic diagram of the experimental arrangement is shown in Fig. 17. A CPM laser operating at 80 GHz repetition rate is used as optical source. The light are coupled into an optical fiber and then amplified by a 1480 nm diode-pumped EDFA. Optical isolators are placed on both sides of the EDFA to prevent reflections back to the CPM laser and to suppress lasing in the EDFA. The wavelength of the CPM laser is designed to be 1.53 μm , matching the gain spectrum of the EDFA. Under normal passive mode-locking conditions, the CPM laser generates pulses with a duration of 1.28 ps, a time-bandwidth product of 0.34,

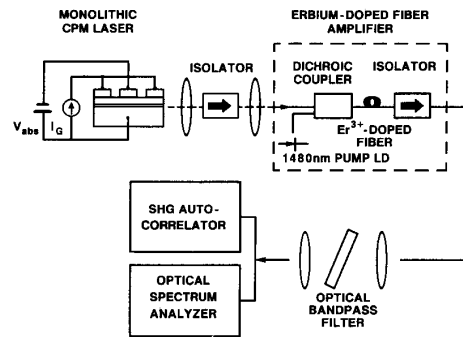


Fig. 17. The experimental arrangement for the tunable monolithic CPM quantum-well laser.

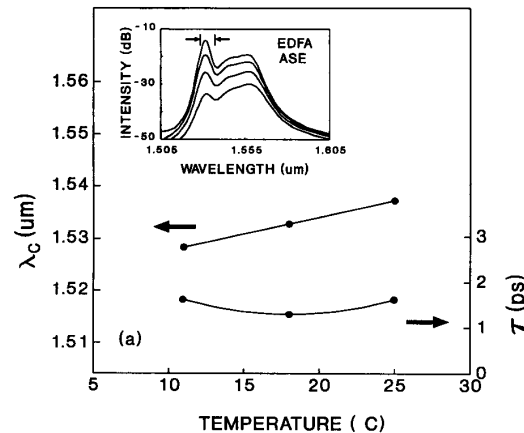


Fig. 18. The center lasing wavelength (λ_c) and the corresponding pulsewidth (τ) of a 1 mm long passive CPM laser for various heat sink temperatures. The inset shows the amplified spontaneous noise spectra of the erbium-doped fiber amplifier under various optical pump power.

and a peak power of 5 mW. The EDFA provides 20 dB gain for an average input power of -8 dBm. The peak power of the amplified pulses is 160 mW.

The center wavelength of the CPM laser can be fine tuned by adjusting the heat-sink temperature. Fig. 18 shows the temperature dependence of the center wavelength (λ_c) and the pulsewidth (τ) from 11 to 25°C. The spectral envelope shifts continuously toward the longer wavelength side with increasing temperature, and λ_c moves from 1528.4 to 1537.2 nm. This tuning range of 8.8 nm is limited by bandwidth of the EDFA gain peak at 1.53 μm . Wider tuning range can be expected if the laser operates at the 1.56 μm plateau of the EDFA. The wavelength tuning rate is 0.63 nm/°C. The pulse has a minimum width of 1.3 ps at 1532.8 nm, which is the gain peak of the EDFA. As the laser wavelength is tuned away from the EDFA gain peak, the spectral bandwidth becomes narrower and the pulsewidth broadens slightly. Larger pulsewidth can be produced by spectral windowing with narrow band-pass filters. Fig. 19 shows the autocorrelation traces and the corresponding optical spectra of the filtered CPM pulses. The pulsewidth is increased

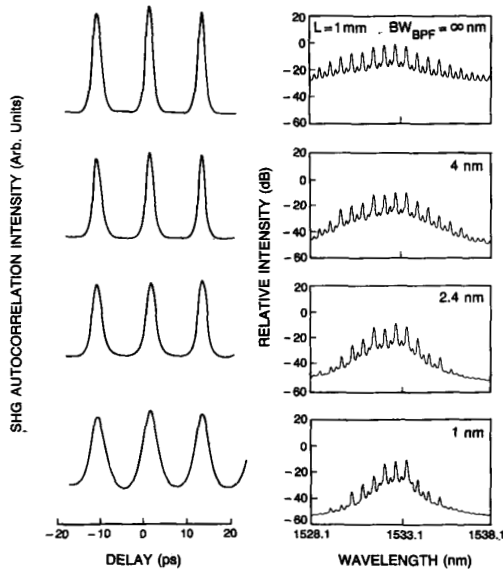


Fig. 19. The autocorrelation traces and the corresponding optical spectra of the filtered CPM pulses for various filter bandwidth. The FWHM pulsewidths of 1.6, 1.8, and 2.9 ps are obtained for filter bandwidths ($\Delta\lambda_{BPF}$) of 4, 2.4, and 1, respectively.

by inserting band-pass filters with various bandwidths ($\Delta\lambda_{BPF}$), and the FWHM widths of 1.6, 1.8, 2.9 ps are obtained for $\Delta\lambda_{BPF} = 4, 2.4$, and 1 nm, respectively. The pulse width can be approximated by

$$\tau = (\tau_0 \Delta\lambda_0) \sqrt{\frac{1}{\Delta\lambda_0^2} + \frac{1}{\Delta\lambda_{BPF}^2}} \quad (1)$$

where τ_0 and $\Delta\lambda_0$ are the pulsewidth and the spectral bandwidth in the absence of the filters, respectively.

VII. MONOLITHIC CPM LASER WITH INTEGRATED GRATING REFLECTORS

The wavelength tuning and bandwidth filtering can be integrated into the monolithic laser cavity using semiconductor processing technology. Integrated Bragg reflectors have been used in the photonic integrated circuits (PIC's) [45] and integrated active mode-locked lasers [46]. We have integrated Bragg reflectors into the cavity to control the emission wavelength as well as the spectral width of monolithic CPM MQW lasers.

The layer structure is depicted in Fig. 20. Grating reflectors are located near the facets. The first-order grating ($\lambda = 1.54 \mu\text{m}$) is defined on the n^+ -InP substrates by holography and shallow chemical etching. Dielectric SiO_2 patterning and mass-transport process are utilized to define the localized gratings. After the SiO_2 mask is removed, the wafer is loaded into the OMVPE reactor and the following layers are grown subsequently: n-type InGaAsP quaternary waveguide layer ($\lambda_g = 1.1 \mu\text{m}$), undoped InGaAsP separate confinement layer ($\lambda_g = 1.2 \mu\text{m}$), undoped four quantum wells, undoped InGaAsP

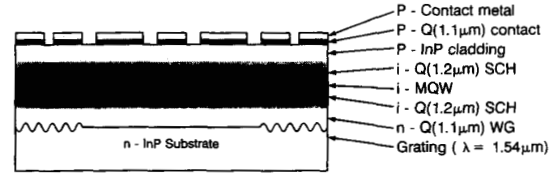


Fig. 20. The layer structure for fabricating monolithic CPM lasers with integrated grating reflectors. Gratings outside the SiO_2 -protected reflector regions are selectively removed by a mass-transport process before the growth of epitaxial layers.

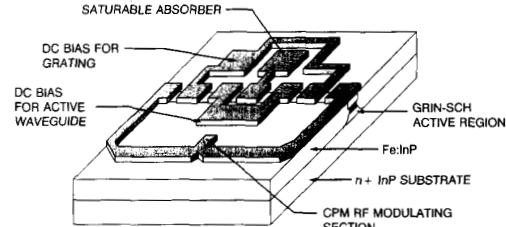


Fig. 21. The schematic diagram of the monolithic CPM laser with integrated grating reflectors.

separate confinement layer ($\lambda_g = 1.2 \mu\text{m}$), p-type InP cladding layer, and p-type InGaAsP contact layer ($\lambda_g = 1.1 \mu\text{m}$). The gain peak of this MQW active region is adjusted to $1.54 \mu\text{m}$ to match the Bragg wavelength of the gratings. Buried heterostructure laser strips are then formed with Fe-doped semi-insulating InP blocking layer. Fig. 21 shows the schematic diagram of the monolithic CPM laser with integrated grating reflectors. The total cavity length is 2.54 mm and its top contact layer is divided into seven sections: a $50 \mu\text{m}$ long saturable absorber at the center of the cavity, two $50 \mu\text{m}$ long modulator sections near the facets, two $200 \mu\text{m}$ long grating sections, and two gain sections for the rest of cavity.

Depending on the dc bias combinations of these sections, the laser operates in one or the combination of Fabry-Perot, distributed feedback (DFB), and CPM lasing modes. Fig. 22 shows the optical spectrum and the corresponding small-signal microwave response of this CPM laser with integrated grating reflectors. In Fig. 22(a), a combination of Fabry-Perot and DFB modes coexist. Its microwave spectrum shows the Fabry-Perot resonant peak at 16.8 GHz together with a DFB resonant peak near 19 GHz. By reverse-biasing the modulator sections to suppress the modal gain of the Fabry-Perot modes and increasing the forward current in the grating sections, a dominant DFB lasing mode with a side-mode suppression ratio greater than 35 dB is observed in the optical spectrum of Fig. 22(b). Under this bias condition, the 16.8 GHz Fabry-Perot resonance disappears from the RF spectrum, and a narrow resonant peak is present at 19 GHz from the DFB mode. The resonant frequency of the DFB mode (19.4 GHz) is higher than that of the Fabry-Perot modes (16.8 GHz) because the effective cavity length of the laser with grating reflectors is shorter than the cavity length defined by the two cleaved facets. By adjusting the

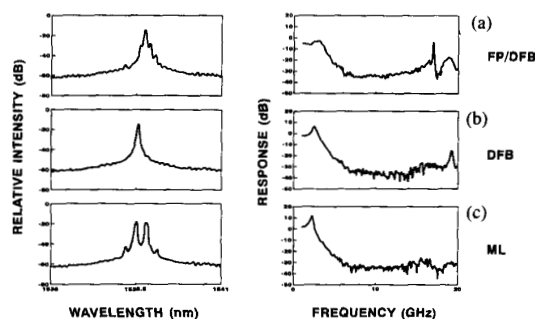


Fig. 22. The optical spectrum and small-signal microwave response of a 2.54 mm long monolithic CPM laser with integrated grating reflectors under (a) mixture of Fabry-Perot and DFB modes, (b) DFB modes, and (c) mode locking.

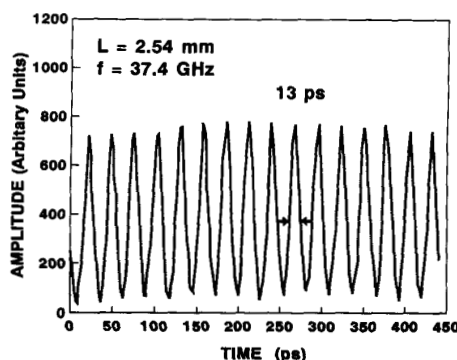


Fig. 23. The temporal trace of a 2.54 mm long CPM laser with integrated grating reflectors taken by a synchron-scan streak camera. The corresponding spectral width is ~ 0.31 nm which is limited by the bandwidth of the gratings.

bias conditions properly, a mode-locked optical output is obtained by phase-locking a group of longitudinal modes inside the stopband of the grating reflectors [Fig. 22(c)]. The width of the stopband is determined by the coupling coefficient of the grating which can be controlled by the depth of the grating and the thickness of the n-type $1.1 \mu\text{m}$ InGaAsP waveguide layer. Fig. 23 shows the temporal response of the CPM laser with integrated grating reflectors when it is driven by a RF oscillator at 37.4 GHz. The FWHM pulsewidth is 13 ps. Because of the active gratings and large κL value used in the current design, only a limited number of cavity modes are locked which result in large pulsewidth. Nevertheless, we demonstrate the controls of the lasing wavelength and spectral width of the monolithic CPM laser by the integrated grating reflectors.

VIII. SUMMARY

In summary, we have exploited the semiconductor laser technology to fabricate compact and reliable monolithic CPM lasers on a single chip to produce subpicosecond transform-limited optical pulses. The pulses are also amplified and tailored by broad-band erbium-doped fiber amplifier, external band-pass filters, and integrated grating

reflectors. This miniature CPM semiconductor laser is very useful for many applications in high bit rate optical communication and computation systems.

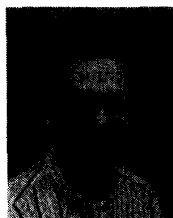
ACKNOWLEDGMENT

The authors would like to acknowledge the excellent OMVPE wafers prepared by Dr. R. A. Logan and Dr. T. Tanbun-Ek, erbium-doped fibers from Dr. J. Simpson, and technical help from M. A. Chin and A. M. Sergent.

REFERENCES

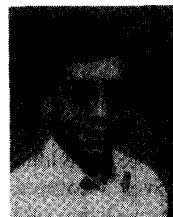
- [1] A. Hasegawa, *Optical solitons in fibers*, 2nd ed. New York: Springer-Verlag, 1990.
- [2] L. F. Mollenauer, S. G. Evangelides, and H. A. Haus, "Long-distance soliton propagation using lumped amplifiers and dispersion shifted fiber," *J. Lightwave Technol.*, vol. 9, pp. 194-197, 1991.
- [3] M. N. Islam, C. E. Socolich, and D. A. B. Miller, "Low-energy ultrashort fiber soliton logic gates," *Opt. Lett.*, vol. 15, pp. 909-911, Aug. 1990.
- [4] N. R. Whitaker, Jr., H. Avramopoulos, P. M. W. French, M. C. Gabriel, R. E. LaMarche, D. J. Digiovanni, and H. M. Presby, "All-optical arbitrary demultiplexing at 2.5 Gb/s with tolerance to timing jitter," *Opt. Lett.*, vol. 16, pp. 1838-1840, 1991.
- [5] B. P. Nelson, K. J. Blow, P. D. Constantine, N. J. Doran, J. K. Lucek, I. W. Marshall, and K. Smith, "All-optical Gbit/s switching using nonlinear optical loop mirror," *Electron. Lett.*, vol. 27, pp. 704-705, 1991.
- [6] J. A. Valdmanis and B. Mourou, "Subpicosecond electrooptic sampling: principles and applications," *IEEE J. Quantum Electron.*, vol. QE-22, pp. 69-78, 1986.
- [7] D. H. Auston and M. C. Nuss, "Electrooptic generation and detection of femtosecond electrical transients," *IEEE J. Quantum Electron.*, vol. 24, pp. 184-197, 1988.
- [8] P. M. Downey, J. E. Bowers, R. S. Tucker, and E. Agyekum, "Picosecond dynamics of a gain-switched InGaAsP laser," *IEEE J. Quantum Electron.*, vol. QE-23, pp. 1039-1047, 1987.
- [9] Y. Arakawa, T. Sogawa, M. Nishioka, M. Tanaka, and H. Sakaki, "Picosecond pulse generation (< 1.8 ps) in a quantum well laser by a gain switch method," *Appl. Phys. Lett.*, vol. 51, pp. 1295-1297, 1987.
- [10] K. Y. Lau, "Gain switching of semiconductor injection lasers," *Appl. Phys. Lett.*, vol. 52, pp. 257-259, 1988.
- [11] T. Koch and J. Bowers, "Nature of wavelength chirping in directly modulated semiconductor lasers," *Electron. Lett.*, vol. 20, pp. 1038-1040, 1984.
- [12] E. H. Bottcher, K. Ketterer, and D. Bimberg, "Turn-on delay time fluctuations in gain switched AlGaAs/GaAs multiple-quantum-well lasers," *J. Appl. Phys. Lett.*, vol. 63, pp. 2469-2471, 1988.
- [13] For an overview, J. P. van der Ziel, "Mode locking of semiconductor lasers," *Semiconductors and Semimetals*, vol. 22, Part B, W. T. Tsang, Ed. Orlando, FL: Academic, 1985, ch. 1.
- [14] P. T. Ho, L. A. Glasser, E. P. Ippen, and H. A. Haus, "Picosecond pulse generation with a cw GaAlAs laser diode," *Appl. Phys. Lett.*, vol. 33, pp. 241-242, 1978.
- [15] J. E. Bowers, P. A. Morton, A. Mar, and S. W. Corzine, "Actively mode-locked semiconductor lasers," *IEEE J. Quantum Electron.*, vol. 25, pp. 1426-1439, 1989.
- [16] K. Lau, "Narrow-band modulation of semiconductor lasers at millimeter wave frequencies (> 100 GHz) by mode-locking," *IEEE J. Quantum Electron.*, vol. 26, pp. 250-261, 1990.
- [17] P. P. Vasilev and A. B. Sergeev, "Generation of bandwidth-limited 2 ps pulses with 100 GHz repetition rate from multi-segmented injection laser," *Electron. Lett.*, vol. 25, pp. 1049-1050, 1989.
- [18] S. Sanders, L. Eng, J. Paslaski, and A. Yariv, "108 GHz passive mode locking of a multiple quantum well semiconductor laser with an intracavity absorber," *Appl. Phys. Lett.*, vol. 56, pp. 310-312, 1990.
- [19] H. A. Haus and H. L. Dyckman, "Timing of laser pulses produced by combined passive and active mode-locking," *Int. J. Electron.*, vol. 44, pp. 225-238, 1978.
- [20] P. A. Morton, J. E. Bowers, L. A. Koszi, M. Soler, J. Lopata, and

- D. P. Wilt, "Monolithic hybrid mode-locked 1.3 μm semiconductor lasers," *Appl. Phys. Lett.*, vol. 56, pp. 111-113, 1990.
- [21] H. A. Haus, "Theory of mode-locking with a slow saturable absorber," *IEEE J. Quantum Electron.*, vol. QE-11, pp. 736-746, 1975; —, "Theory of mode-locking with a fast saturable absorber," *J. Appl. Phys.*, vol. 46, pp. 3049-3058, 1975; —, "Parameter ranges for cw passive mode-locking," *IEEE J. Quantum Electron.*, vol. QE-12, pp. 169-176, 1976.
- [22] R. L. Fork, B. I. Greene, and C. V. Shank, "Generation of optical pulses shorter than 0.1 ps by colliding pulse mode locking," *Appl. Phys. Lett.*, vol. 38, pp. 671-672, 1981.
- [23] C. V. Shank, "Generation of ultrashort optical pulses," in *Ultrashort Laser Pulses and Applications*, W. Kaiser, Ed., Berlin: Springer-Verlag, 1988, ch. 2, pp. 5-34.
- [24] E. M. Garmire and A. Yariv, *IEEE J. Quantum Electron.*, vol. QE-3, p. 222, 1967.
- [25] M. S. Stix and E. P. Ippen, "Pulse shaping in passively mode-locked ring dye laser," *IEEE J. Quantum Electron.*, vol. 19, pp. 520-525, 1983.
- [26] J. P. van der Ziel, R. A. Logan, and R. M. Mikulyak, "Generation of subpicosecond pulses from an actively mode-locked GaAs laser in an external cavity," *Appl. Phys. Lett.*, vol. 39, pp. 867-869, 1981.
- [27] P. P. Vasilev, V. N. Morozov, Y. M. Popov, and A. B. Sergeev, "Subpicosecond pulse generation by a tandem-type AlGaAs DH laser with colliding pulse mode locking," *IEEE J. Quantum Electron.*, vol. 22, pp. 149-152, 1986.
- [28] R. S. Tucker, U. Koren, G. Raybon, C. A. Burrus, B. I. Miller, T. L. Koch, G. Eisenstein, and A. Shahar, "40 GHz active mode-locking in a 1.5 μm monolithic extended-cavity laser," *Electron. Lett.*, vol. 25, pp. 622-623, 1989.
- [29] Y. Silberberg, P. M. Smith, D. J. Eilenberger, D. A. B. Miller, A. C. Gossard, and W. Weigmann, "Passive mode locking of a semiconductor diode laser," *Opt. Lett.*, vol. 9, pp. 507-509, 1984.
- [30] Y. Arakawa and A. Yariv, "Quantum well lasers—gain spectra, dynamics," *IEEE J. Quantum Electron.*, vol. QE-22, pp. 1887-1899, 1987.
- [31] For reviews, W. T. Tsang, in *Semiconductor and semimetals*, R. Dingle, Ed., Orlando, FL: Academic, 1987, vol. 24, ch. 7.
- [32] W. H. Knox, R. L. Fork, M. C. Downer, D. A. B. Miller, D. S. Chemla, C. V. Shank, A. C. Gossard, and W. Weigmann, *Phys. Rev. Lett.*, vol. 54, p. 1306, 1985; or D. S. Chemla and D. A. B. Miller, *J. Opt. Soc. Amer. B*, vol. 2, pp. 1155-1158, 1985.
- [33] P. J. Delfyett, C. H. Lee, L. T. Florez, N. G. Stoffel, T. J. Gmitter, N. C. Andreadakis, G. A. Alphonse, and J. C. Connolly, "Generation of subpicosecond high-power optical pulses from a hybrid mode-locked semiconductor laser," *Opt. Lett.*, vol. 15, pp. 1371-1373, 1990.
- [34] W. Xiang, S. R. Friberg, K. Watanabe, S. Machida, W. Jiang, H. Iwamura, and Y. Yamamoto, "Femtosecond external-cavity surface-emitting InGaAs/InP multiple-quantum-well laser," *Opt. Lett.*, vol. 16, pp. 1394-1396, 1991.
- [35] K. L. Hall, J. Mark, E. P. Ippen, and G. Eisenstein, "Femtosecond gain dynamics in InGaAsP optical amplifiers," *Appl. Phys. Lett.*, vol. 56, pp. 1740-1742, 1990.
- [36] G. Eisenstein, J. M. Weisenfeld, M. Wegener, G. Sucha, D. S. Chemla, S. Weiss, G. Raybon, and U. Koren, "Ultrafast gain dynamics in 1.5 μm multiple quantum well optical amplifiers," *Appl. Phys. Lett.*, vol. 58, pp. 158-160, 1991.
- [37] C. T. Hultgren and E. P. Ippen, "Ultrafast refractive index dynamics in AlGaAs diode laser amplifiers," *Appl. Phys. Lett.*, vol. 59, pp. 635-637, 1991.
- [38] S. Weiss, J. M. Weisenfeld, D. S. Chemla, G. Raybon, G. Sucha, M. Wegener, G. Eisenstein, C. A. Burrus, A. G. Dentai, U. Koren, B. I. Miller, H. Temkin, R. A. Logan, and T. Tanbun-Ek, "Carrier capture times in 1.5 μm multiple quantum well optical amplifiers," *Appl. Phys. Lett.*, vol. 60, pp. 9-11, 1992.
- [39] T. Tanbun-Ek, R. A. Logan, H. Temkin, K. Berthold, A. F. J. Levi, and S. N. G. Chu, "Very low threshold InGaAs/InGaAsP graded index separate confinement heterostructure quantum well lasers grown by atmospheric pressure metalorganic vapor phase epitaxy," *Appl. Phys. Lett.*, vol. 55, pp. 2283-2285, 1989.
- [40] Y. K. Chen, M. C. Wu, T. Tanbun-Ek, R. A. Logan, and M. A. Chin, "Subpicosecond monolithic colliding-pulse mode-locked multiple quantum well lasers," *Appl. Phys. Lett.*, vol. 58, pp. 1253-1255, 1991.
- [41] M. C. Wu, Y. K. Chen, T. Tanbun-Ek, R. A. Logan, M. A. Chin, and G. Raybon, "Transform-limited 1.4 ps optical pulses from a monolithic colliding-pulse mode-locked quantum well laser," *Appl. Phys. Lett.*, vol. 57, pp. 759-761, 1990.
- [42] K. Y. Lau and J. Paslaski, "Condition for short pulse generation in ultrahigh frequency mode-locking of semiconductor lasers," *IEEE Photon. Technol. Lett.*, vol. 3, pp. 974-976, 1991.
- [43] J. Paslaski and K. Y. Lau, "Parameter ranges for ultrahigh frequency mode-locking of semiconductor lasers," *Appl. Phys. Lett.*, vol. 59, pp. 7-9, 1991.
- [44] R. J. Mears, L. Reekie, I. M. Jauncey, and D. N. Payne, "Low-noise erbium-doped fibre amplifier operating at 1.54 μm ," *Electron. Lett.*, vol. 23, pp. 1026-1028, 1987.
- [45] T. Koch and U. Koren, "Semiconductor photonics integrated circuits," *IEEE J. Quantum Electron.*, vol. 27, pp. 641-654, 1991.
- [46] P. B. Hansen, G. Raybon, U. Koren, B. I. Miller, M. G. Young, M. Chien, C. A. Burrus, and R. C. Alfemess, "5.5-mm long InGaAsP monolithic extended-cavity laser with an integrated Bragg-reflector for active mode-locking," *IEEE Photon. Technol. Lett.*, vol. 4, pp. 215-217, 1992.



Young-Kai Chen (S'76-M'80) received the bachelor degree in electronics engineering from National Chiao Tung University, Hsinchu, Taiwan, in 1976, the M.S.E.E. degree from Syracuse University, Syracuse, NY, in 1980, and the Ph.D. degree from Cornell University, Ithaca, NY, in 1988.

From 1980 to 1985, he was a member of the Technical Staff in the Electronics Laboratory of General Electric Company, Syracuse, NY, working on the modeling and design of silicon and GaAs integrated circuits for phase array applications. From 1985 to 1988, he was working on his doctoral research on high frequency nanometer-gate heterostructure transistors at Cornell University and also working as a consultant with General Electric Co. Since February 1988, he has been with Solid-State Electronics Research Laboratory of AT&T Bell Laboratories, Murray Hill, NJ, as a member of the Technical Staff. His research interests center on high-frequency compound semiconductor optoelectronic devices and integrated circuits, nonequilibrium carrier transport dynamics in reduced-dimensional transistors, and ultrafast optoelectronic processes in semiconductors.



Ming C. Wu (S'80-M'88) was born in Taipei, Taiwan, on November 13, 1960. He received the B.S. degree in electrical engineering from National Taiwan University in 1983 and the M.S. and Ph.D. degrees in electrical engineering and computer sciences from the University of California, Berkeley, in 1985 and 1988, respectively.

He joined the Semiconductor Electronics Research Department of AT&T Bell Laboratories, Murray Hill, NJ, as a member of the Technical Staff in 1988. His research interests include high-speed optoelectronic devices for optical communication and computing, nanofabrication of tunable single-frequency lasers, ultrashort optical pulse generation in quantum-well lasers, and ultrafast phenomena in semiconductors.

Dr. Wu is a member of the Optical Society of America, the IEEE Lasers and Electro-Optics Society, and the American Physical Society.